ABILITIES OF WAVELET ANALYSIS FOR INVESTIGATING SHORT-PERIOD VARIATIONS OF EARTH ROTATION

Michael Schmidt, Harald Schuh - Deutsches Geodätisches Forschunginstitut, (DGFI)
Marstallplatz 8 - D-80539 München, Germany
E-mail: schmidt@dgfi.badw.de

1 INTRODUCTION

In the last decade the sub-seasonal variations of polar motion and length of day containing oscillations with periods shorter than half a year have been investigated and their time variations have been found. Correlations in the time domain between sub-seasonal variations of Earth rotation and sub-seasonal variations of effective atmospheric angular momentum functions were determined and studied. A comprehensive list of references is given by KOLACZEK et al. (2000).

Today, besides the standard Fourier analysis of which the foundations will be given in the second section of this paper, the wavelet analysis is a very powerful method for analysing time series such as Earth rotation data. In the main part of the paper the wavelet cross-covariance function, the wavelet cross-scalogram, the wavelet cross-correlation function and the normed coherency will be defined. These are excellent tools for the comparison of polar motion and length of day (LOD) time series with atmospheric angular momentum (AAM) time series. Examples will be given for the short-period range, i.e. for periods between 5 and 150 days (for LOD) and between 5 and 60 days (for polar motion).

2 FOURIER ANALYSIS

First we assume that a wide sense stationary and ergodic time series or stochastic signal $x(t)$ is observed within the time intervall $T = t_2 - t_1$ with $t_1 \leq t \leq t_2$. Generally, a process is called *stationary* if the mean or *expected value function* $E\big[x(t)\big] = \mu_x$ is a constant and the *autocovariance function* $E\big[(x^*(t_1) - \mu_x^*)\ (x(t_2) - \mu_x)\big] = C_x(\tau)$ depends only on the time difference $\tau = t_2 - t_1$. Without loss of generality we assume that the signal $x(t)$ is of zero mean. Thus, the *Fourier transform* reads

$$X_T(j\omega) = \int_T x(t)\, e^{-j\omega t}\, dt\,. \tag{2.1}$$

Estimations $\tilde{C}_x(\tau)$ and $\tilde{S}_x(\omega)$ of the autocovariance function $C_x(\tau)$ and the *Fourier spectrum* $S_x(\omega)$ are given by

$$\tilde{C}_x(\tau) = \frac{1}{T} \int_{t_1}^{t_2-\tau} x^\star(t)\, x(t+\tau)\, dt\,, \tag{2.2}$$

$$\tilde{S}_x(\omega) = \frac{1}{T} \left|X_T(j\omega)\right|^2 \tag{2.3}$$

with $\tilde{C}_x(-\tau) = \tilde{C}_x^\star(\tau)$ for $0 \le \tau \le T$. $x^\star(t)$ denotes the conjugate complex function of $x(t)$. Analogously to the time series $x(t)$ we introduce the stationary and ergodic signal $y(t)$ with the expected value function $\mu_y = 0$ and the autocovariance function $E\big[y^\star(t)\, y(t+\tau)\big] = C_y(\tau)$. An estimation $\tilde{S}_{x,y}(j\omega)$ of the *Fourier cross-spectrum* $S_{x,y}(j\omega)$ is given by

$$\tilde{S}_{x,y}(j\omega) = \int_{-T}^{T} \tilde{C}_{x,y}(\tau)\, e^{-j\omega\tau}\, d\tau = \frac{1}{T}\, X_T^\star(j\omega)\, Y_T(j\omega)\,, \tag{2.4}$$

where the function

$$\tilde{C}_{x,y}(\tau) = \frac{1}{T} \int_{t_1}^{t_2-\tau} x^\star(t)\, y(t+\tau)\, dt \tag{2.5}$$

with $\tilde{C}_{x,y}(-\tau) = \tilde{C}_{y,x}^\star(\tau)$ and $0 \le \tau \le T$ is an estimation of the *cross-covariance function* $C_{x,y}(\tau)$. The complex-valued function

$$\Gamma_{x,y}(j\omega) = \frac{S_{x,y}(j\omega)}{\big(S_x(\omega)\, S_y(\omega)\big)^{1/2}} \tag{2.6}$$

with $0 \le |\Gamma_{x,y}(j\omega)| \le 1$ is a measure for the similarity of the two processes $x(t)$ and $y(t)$ in dependence on the angular frequency ω.

3 MORLET WAVELET ANALYSIS

The *continuous wavelet transform* of the stationary stochastic signal $x(t)$ - introduced in the last section - is defined by

$$X_T(b,a) = \int_T x(t)\, \psi_{a,b}^\star(t)\, dt\,, \tag{3.1}$$

where a denotes the *scale parameter* and b the *shift parameter.* The functions

$$\psi_{a,b}(t) = |a|^{-1/2}\, \psi\Big(\frac{t-b}{a}\Big) \tag{3.2}$$

are computed from the wavelet function $\psi(t)$ which is restricted to the admissibility condition $\int_{\mathbb{R}} \psi(t)\, dt = 0$. In geodetic and geophysical applications the complex-valued *Morlet wavelet function*

$$\psi(t) = e^{j\omega_0 t}\, \big(\, e^{-t^2/2\sigma^2} - 2\, e^{-\omega_0^2\sigma^2/4}\, e^{-t^2/\sigma^2}\,\big) \tag{3.3}$$

is often used. If we choose $\omega_0 = 2\pi$ for the constant ω_0 the value of the scale parameter a is approximately equal to the period time $\frac{2\pi}{\omega}$; see e.g. (SCHMIDT 1996). The constant $\sigma \ge 1$ defines the shape of the envelope of the Morlet wavelet function. Because of the admissibility condition the expected value function of the wavelet transform of a stationary signal is always

equal zero. Thus, an estimation of the autocovariance function $E\big[X^\star(b_1,a)\,X(b_2,a)\big] = C_X(\beta,a)$ of the wavelet transform is given by

$$\tilde{C}_X(\beta,a) = \int_{-T}^{T} \tilde{C}_x(\tau)\,\zeta^\star_{a,\beta}(\tau)\,d\tau \tag{3.4}$$

where $\beta = b_2 - b_1$ is the difference between the two values b_1 and b_2 for the shift parameter b (SCHMIDT 2000). The so-called *zeta-functions*

$$\zeta_{a,\beta}(\tau) = \int_{\mathbb{R}} \psi_{a,\beta}(t)\,\psi^\star_{a,\tau}(t)\,dt = \zeta\Big(\frac{\tau-\beta}{a}\Big) \tag{3.5}$$

are computed from the wavelet function $\psi(t)$. Because of the fact that the function $\zeta(\tau)$ satisfies the admissibility condition, we conclude from equation (3.4) that the autocovariance function $C_X(\beta,a)$ of the wavelet transform (3.1) is obtained by a wavelet transform of the autocovariance function $C_x(\tau)$ by means of the wavelet function $\zeta(\tau)$. In the case of the Morlet wavelet function (3.3) the zeta function reads approximately

$$\zeta(\tau) = \sqrt{\pi}\,\sigma\,e^{j\omega_0\tau}\;e^{-\tau^2/4\sigma^2}\;. \tag{3.6}$$

Besides formula (3.4) a second representation of the estimated autocovariance function $\tilde{C}_X(\beta,a)$ is given by

$$\tilde{C}_X(\beta,a) = \frac{1}{T}\int_{\mathbb{R}} X^\star_T(b,a)\,X_T(b+\beta,a)\,db \tag{3.7}$$

(SCHMIDT 2000). Thus, for $\beta = 0$ the *wavelet scalogram*

$$W_x(b,a) = |X_T(b,a)|^2 \tag{3.8}$$

may be interpreted as the *energy density function* depending on the shift parameter b and the scale parameter a; see e.g. (KUMAR and FOUFOULA-GEORGIOU 1994, p.13).

Again we introduce a second stationary stochastic signal $y(t)$ and define - corresponding to the equations (3.4) and (3.7) - the estimation

$$\tilde{C}_{X,Y}(\beta,a) = \int_{-T}^{T} \tilde{C}_{x,y}(\tau)\,\zeta^\star_{a,\beta}(\tau)\,d\tau = \frac{1}{T}\int_{\mathbb{R}} X^\star_T(b,a)\,Y_T(b+\beta,a)\,db \tag{3.9}$$

of the *cross-covariance function* $C_{X,Y}(\beta,a)$. According to (3.1) $Y_T(b,a)$ denotes the wavelet transform of the process $y(t)$. Analogously to (3.8) the complex-valued function

$$W_{x,y}(b,a) = X^\star_T(b,a)\,Y_T(b,a) \tag{3.10}$$

is called the *wavelet cross-scalogram*. Finally we define the *cross-correlation function*

$$\rho_{X,Y}(\beta,a) = \frac{C_{X,Y}(\beta,a)}{\sigma_X(a)\,\sigma_Y(a)} \tag{3.11}$$

with $0 \le |\rho_{X,Y}(\beta,a)| \le 1$ depending on the difference $\beta = b_2 - b_1$ and the scale parameter a. For $\beta = 0$ the square of the cross-correlation function $\rho_{X,Y}(0,a) = \Gamma_{X,Y}(a)$ is denoted as the *normed coherency* of the wavelet transform. Estimates for the cross-covariance function $C_{X,Y}(\beta,a)$ and the variances $C_X(0,a) = \sigma^2_X(a)$ and $C_Y(0,a) = \sigma^2_Y(a)$ are calculated from the equations (3.7) and (3.9), respectively.

4 NUMERICAL EXAMPLES

If the value of the square $|W_{x,y}(b,a)|^2 = W_x(b,a)\,W_y(b,a)$ of the wavelet cross-scalogram (3.10) is equal to zero, we cannot decide whether only one of the wavelet scalograms $W_x(b,a)$ and $W_y(b,a)$ is zero or both. Thus, the process of comparing two signals $x(t)$ and $y(t)$ includes the computation both the squared cross-scalogram and the normed coherency defined in the context of equation (3.11). This will be demonstrated by the following examples, which are based on the data sets of *length of day (LOD)*, *polar motion* and *atmospheric angular momentum (AAM)*. LOD and polar motion were taken from the IERS C04 series for the years 1980 till 1998. The corresponding AAM series derived from global meteorological data by NCEP (National Center for Environmental Prediction) was also provided by IERS (series aam.ncep.reanalysis.1958.1999).

In the first example we compare the LOD-data set with the χ_3-data set of AAM. In the second example polar motion

$$x(t) = x_1(t) - j\,x_2(t) \tag{4.1}$$

is compared with the AAM-data sets of χ_1 and χ_2 combined to the complex function

$$y(t) = \chi_1(t) + j\,\chi_2(t)\,. \tag{4.2}$$

$x_1(t)$ and $x_2(t)$ are the time series of the pole coordinates. The minus sign in (4.1) has to be considered because of the orientation of the coordinate system. The procedure is divided into three parts: First we compute the wavelet scalograms $W_x(b,a)$ and $W_y(b,a)$ of the two signals. In the next step we calculate the square of the wavelet cross-scalogram $W_{x,y}(b,a)$ as the product of the two scalograms. Finally, the normed coherency $|\Gamma_{X,Y}(a)|^2$ is computed. The results - calculated with $\omega_0 = 2\pi$ and $\sigma = 2$ for the constants in the Morlet wavelet function (3.3) and the zeta function (3.6) - are visualized in the figures 1 to 3 and can be summarized by:

1. Comparison of LOD with χ_3-data set (fig. 1): There is obviously a very good agreement of the wavelet scalograms for periods longer than 35 days. The normed coherency amounts more than 0.9; further peaks are detected clearly at 20 days with a normed coherency of ~ 0.6 and at 10 days with a normed coherency of ~ 0.2.

2. Comparison of polar motion with χ_1-, χ_2-data sets (fig. 2,3): The results are presented below in table 1.

prograde motions		retrograde motions	
period [d]	nor. coherency	period [d]	nor. coherency
48	~ 0.54	-58	~ 0.42
38	~ 0.52	-42	~ 0.43
29	~ 0.42	-20	~ 0.55
17	~ 0.35	-14	~ 0.44
9	~ 0.20	-8	~ 0.30

Table 1: Results of comparison between polar motion and AAM time series

5 CONCLUSIONS

When interpreting the figures 1-3 the following conclusions can be drawn:

1. The irregular short-period variations of LOD between 35 days and 150 days are mainly caused by atmospheric excitations; the normed coherency is between 0.90 and 0.96 (see fig. 1).

2. Atmospheric influences with periods as short as 20 days and 10 days on LOD can be seen, which is demonstrated by a normed coherency of 0.6 and 0.2, respectively (see fig. 1).

3. The irregular short-period variations of polar motion are partially caused by atmospheric excitations (maxima at prograde periods of 48, 38, 29, 17 and 9 days and retrograde periods of -58, -42, -20, -14 and -8 days) with a normed coherency between 0.2 and 0.55 (see fig. 2,3).

4. The variations with very short periods (shorter than ± 25 days) are bigger in AAM than in polar motion (relative to long periods) (see fig. 2,3).

5. For the very short periods (shorter than ± 25 days) the retrograde polar motions are comparatively bigger than the prograde motions. This can be seen even better when those parts of the wavelet scalograms (fig. 2,3) i.e. for periods shorter than ± 25 days are plotted only (not shown here).

6. A considerable fraction of the very short retrograde polar motions is caused by atmospheric excitation which can be derived from the relatively high normed coherencies in the period range shorter than -25 days. According to table 1 the biggest value for the normed coherency between the polar motion and the AAM series is obtained for retrograde motions with a period of -20 days (normed coherency ~ 0.55).

7. In future we will consider scale-dependent time delays between the observed data sets and the excitation functions according to equation (3.9).

REFERENCES

KOLACZEK, B., KOSEK, W. and H. SCHUH (2000) Short-period oscillations of Earth rotation. In: DICK, S. (ed.) Proc of the IAU Colloquium 178 Polar Motion: Historical and scientific problems, Cagliari, Sept. 1999, published by the Astronomical Society of the Pacific (in press)

KUMAR, P. and E. FOUFOULA-GEORGIOU (1994) Wavelet Analysis in Geophysics: An Introduction. In: FOUFOULA-GEORGIOU, E. and P. KUMAR (ed.) Wavelets in Geophysics. Academic Press, San Diego

SCHMIDT, M. (1996) Moderne Methoden der Signalanalyse. Z Vermessungswesen 121:315-325

SCHMIDT, M. (2000) Wavelet analysis of stochastic signals. IERS Technical Note No 28

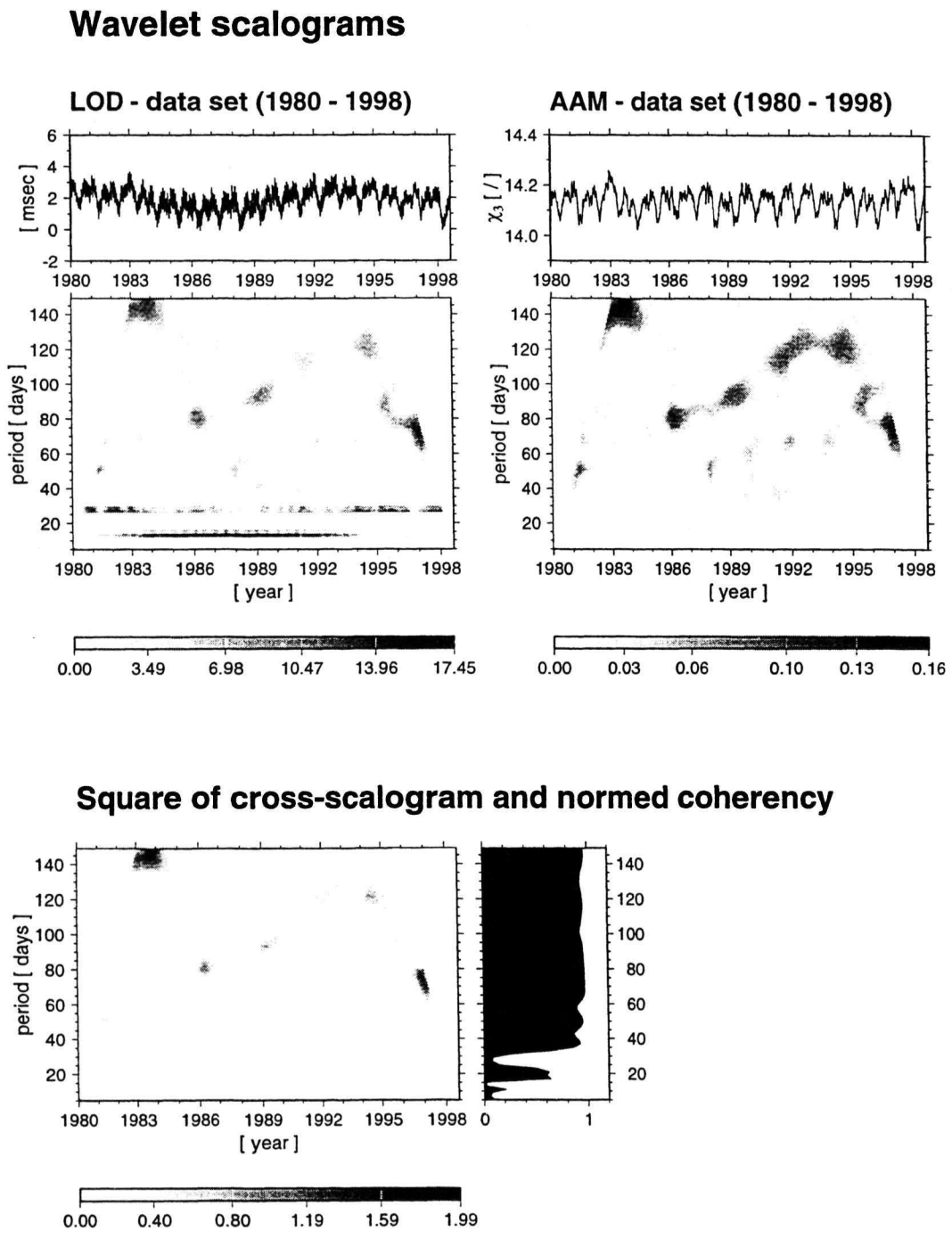

Figure 1: Comparison of LOD-data set with AAM χ_3-data set

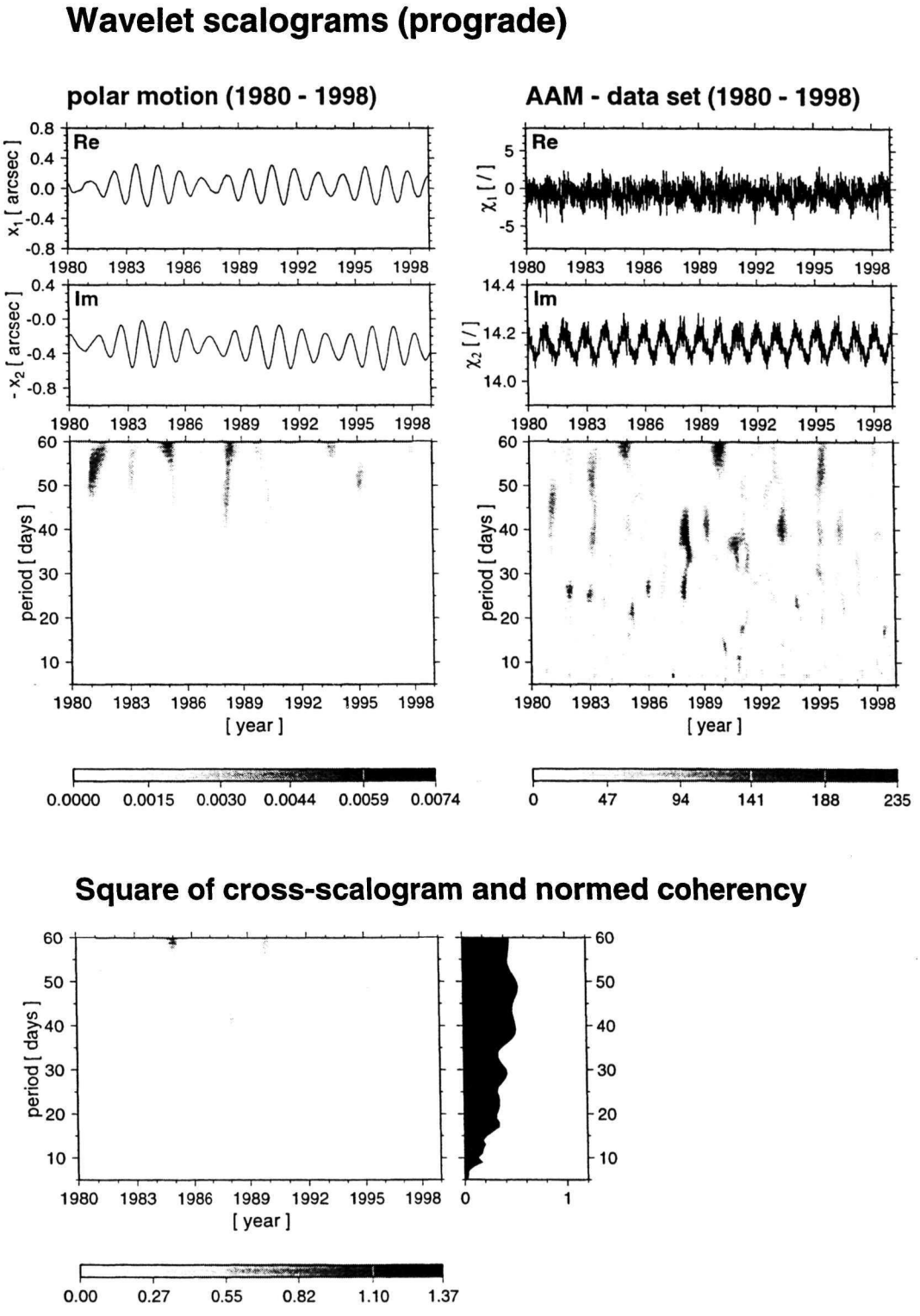

Figure 2: Comparison of polar motion with AAM χ_1-, χ_2-data sets (prograde)

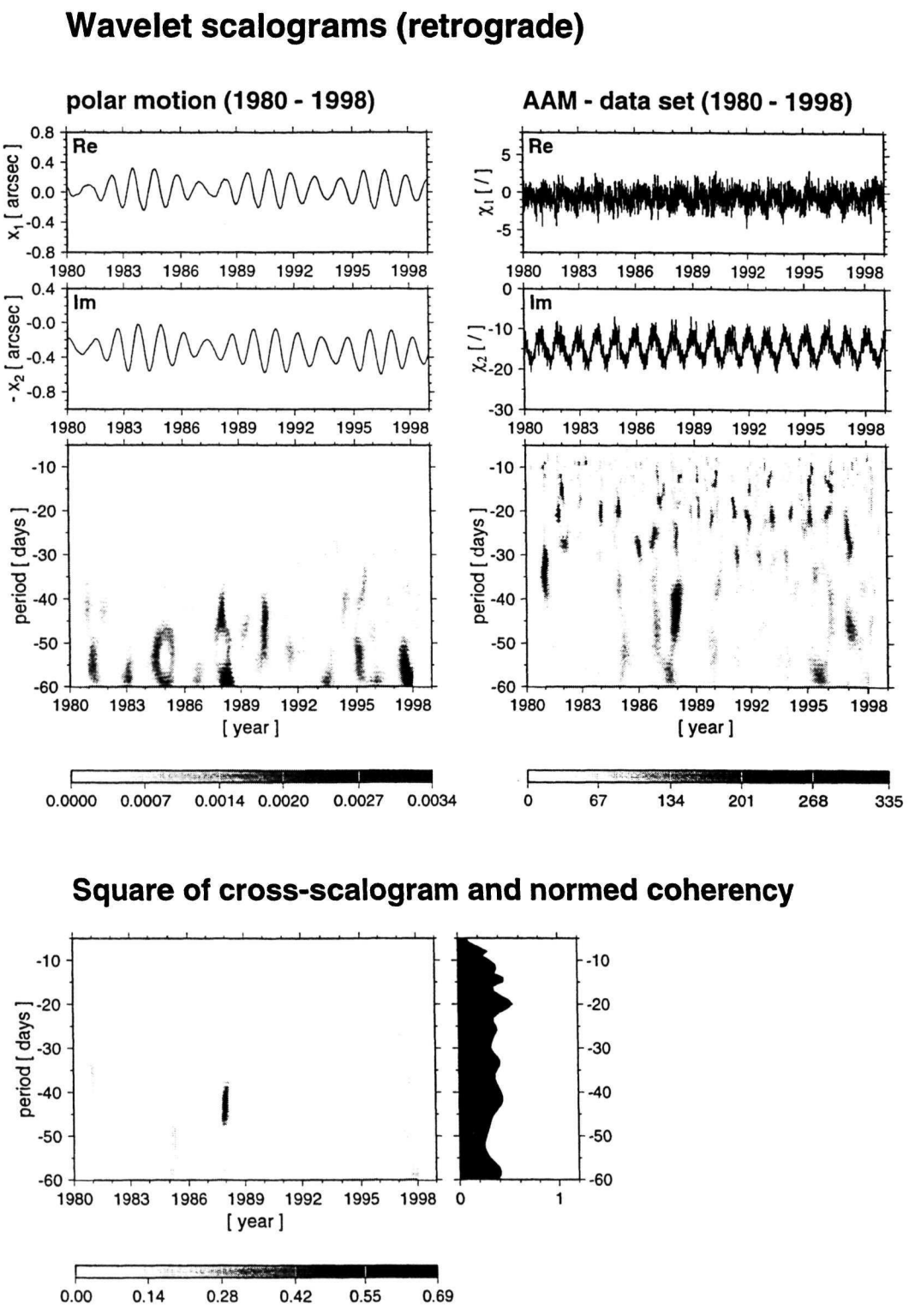

Figure 3: Comparison of polar motion with AAM χ_1-, χ_2-data sets (retrograde)